Chronic oxidative stress compromises telomere integrity and accelerates the onset of senescence in human endothelial cells

David J. Kurz[1,3,*], Stephanie Decary[1,*], Ying Hong[1,2], Elisabeth Trivier[1], Alexander Akhmedov[3] and Jorge D. Erusalimsky[1,2,‡]

[1]Department of Medicine, University College London, 5 University Street, London, WC1E 6JF, UK
[2]The Wolfson Institute for Biomedical Research, University College London, The Cruciform Building, Gower Street, London, WC1E 6BT, UK
[3]Cardiovascular Research, Institute of Physiology, University of Zurich, Winterthurerstr. 190, CH-8057 Zurich, Switzerland
*These authors contributed equally to this work
‡Author for correspondence (e-mail: j.erusalimsky@ucl.ac.uk)

Accepted 9 January 2004
Journal of Cell Science 117, 2417-2426 Published by The Company of Biologists 2004
doi:10.1242/jcs.01097

Summary

Replicative senescence and oxidative stress have been implicated in ageing, endothelial dysfunction and atherosclerosis. Replicative senescence is determined primarily by telomere integrity. In endothelial cells the glutathione redox-cycle plays a predominant role in the detoxification of peroxides. The aim of this study was to elucidate the role of the glutathione-dependent antioxidant system on the replicative capacity and telomere dynamics of cultured endothelial cells. Human umbilical vein endothelial cells were serially passaged while exposed to regular treatment with 0.1 μM *tert*-butyl hydroperoxide, a substrate of glutathione peroxidase, or 10 μM L-buthionine-[S,R]-sulphoximine, an inhibitor of glutathione synthesis. Both treatments induced intracellular oxidative stress but had no cytotoxic or cytostatic effects. Nonetheless, treated cultures entered senescence prematurely (30 versus 46 population doublings), as determined by senescence-associated β-galactosidase staining and a sharp decrease in cell density at confluence. In cultures subjected to oxidative stress terminal restriction fragment (TRF) analysis demonstrated faster telomere shortening (110 versus 55 bp/population doubling) and the appearance of distinct, long TRFs after more than 15-20 population doublings. Fluorescence in situ hybridisation analysis of metaphase spreads confirmed the presence of increased telomere length heterogeneity, and ruled out telomeric end-to-end fusions as the source of the long TRFs. The latter was also confirmed by Bal31 digestion of genomic DNA. Similarly, upregulation of telomerase could not account for the appearance of long TRFs, as oxidative stress induced a rapid and sustained decrease in this activity. These findings demonstrate a key role for glutathione-dependent redox homeostasis in the preservation of telomere function in endothelial cells and suggest that loss of telomere integrity is a major trigger for the onset of premature senescence under mild chronic oxidative stress.

Key words: Ageing, Endothelium, Oxidative stress, Glutathione, Telomere, Telomerase

Introduction

Diseases of the vascular system have long been considered to be age-related in terms of their onset and progression (Lakatta and Levy, 2003). Ageing is associated with endothelial dysfunction (Celermajer et al., 1994; van der Loo et al., 2000; Weinsaft and Edelberg, 2001), impaired angiogenesis (Rivard et al., 1999), defective vascular repair (Weinsaft and Edelberg, 2001) and with an increasing prevalence of atherosclerosis (Strong and McGill, 1962; Weingand et al., 1986). The reasons for these associations are still unclear, but it is plausible that organismal ageing and vascular disease may share common cellular mechanisms. One phenomenon that has been increasingly implicated both in ageing and in the development of vascular pathologies is cellular replicative senescence. The replicative senescence hypothesis proposes that ageing in vivo is related to the limited replicative capacity that normal somatic cells show in vitro (Hayflick, 1965). Replicative senescence entails an irreversible arrest of cell proliferation along with selective changes in differentiated functions (Campisi, 1996). At the mechanistic level, replicative senescence has been linked to the erosion of telomeres (Campisi et al., 2001). These are high order structures formed by specific DNA sequences and a complex array of specialised proteins that cap and stabilise the physical ends of the chromosomes (Blackburn, 2001). In mammals, telomeric DNA consist of tandem hexanucleotide repeats of the sequence TTAGGG, which extend over several thousand base pairs (bp) in length and end in a G-rich single stranded 3′-overhang. Telomeres fold back on themselves to form a loop known as the T-loop that provides functional stability to the telomere, possibly by intercalating the single strand overhang into the double-stranded region of the telomere with the aid of several specialised telomere-related proteins. Telomeric DNA is synthesised by a specialised reverse transcriptase called telomerase (reviewed by Collins and Mitchell, 2002), an enzyme whose expression levels play an important role in determining the onset of

replicative senescence (Bodnar et al., 1998). In the absence of telomerase or when this enzyme is expressed at very low levels, DNA synthesis during cell division results in the progressive shortening of telomeric DNA. This erosion eventually compromises telomere integrity, triggering senescence by activating DNA damage checkpoints that block further cell replication (Smogorzewska and de Lange, 2002).

The progressive oxidative damage of macromolecules resulting from the continual exposure of cellular components to oxidative stress is another process that has long been implicated in ageing and age-related pathologies (reviewed by Finkel and Holbrook, 2000). Interestingly, a substantial body of evidence, mostly from work in fibroblasts, indicates that oxidative stress can also induce or accelerate the development of replicative senescence (reviewed by Serrano and Blasco, 2001). This phenomenon has been collectively termed 'stress-induced premature senescence' (Toussaint et al., 2000). In some studies this early onset of senescence has been attributed to accelerated telomere attrition (reviewed by von Zglinicki, 2002), most probably resulting from the generation of single strand breaks in the telomeric DNA (Petersen et al., 1998). Other reports claim that stress-induced premature senescence may not be related to telomere damage (Chen et al., 2001; Toussaint et al., 2002). It is not clear, however, whether these differences are the result of the cell type under study, the type and level of oxidative insult to which the cells were subjected, the degree of antioxidant protection that the cells could exert, and/or to some other experimental differences.

Human endothelial cells have been shown to be more susceptible to oxidative stress than fibroblasts, which results from substantial differences in the make-up of their antioxidant defence mechanisms (Michiels et al., 1990). In endothelial cells the glutathione redox-cycle plays a predominant role as an anti-oxidant defence against peroxides in general (Suttorp et al., 1986) and against homocysteine-induced oxidative stress in particular (Dayal et al., 2002). Therefore an imbalance in this system may have important implications for the onset of endothelial cell senescence in various pathophysiological contexts related to vascular disease, including hypercholesterolaemia, diabetes mellitus, hyperhomocysteinaemia and chronic inflammation. In this study we demonstrated that long-term exposure of human endothelial cells to mild oxidative stress caused by perturbation of the glutathione redox-cycle results in accelerated telomere erosion, loss of telomeric integrity and the premature onset of replicative senescence.

Materials and Methods

Materials

Human umbilical vein endothelial cells (HUVEC) and endothelial cell growth medium 2 (EGM-2) were purchased from Biowhittaker (Wokingham, UK). *Tert*-butyl hydroperoxide (*t*-BHP) and L-buthionine-[S,R]-sulphoximine (BSO) were from Sigma. Stock solutions of *t*-BHP and BSO were freshly made in water and diluted in medium immediately before addition to the cultures. All other reagents were from standard suppliers or as listed in the text.

Cell culture and pro-oxidant treatments

First passage cryopreserved HUVEC were grown in EGM-2 and serially passaged until they reached senescence, as previously described (Kurz et al., 2000). The number of population doublings (PD) was calculated using the formula PD=(*ln*[number of cells harvested] – *ln*[number of cells seeded]) / *ln*2. To induce oxidative stress, from the second passage onwards parallel cultures were grown in EGM-2 lacking ascorbic acid and exposed at each passage to 0.1 μM *t*-BHP or 10 μM BSO. These compounds were added to the culture medium 48 hours after seeding and then every 2-3 days at the time of feeding. Pro-oxidant treatments were carried out on five independent cultures (three times with *t*-BHP, two times with BSO) from two batches of genetically distinct single donor HUVEC, and unless otherwise indicated results from one representative experiment are shown.

Viability assay

Viability was assessed by flow cytometry using dual staining with calcein-AM and ethidium homodimer-1 (Molecular Probes, OR, USA) as previously described (Levesque et al., 1995).

Measurement of intracellular pro-oxidant capacity

Early passage HUVEC were seeded into 96-well plates at a density of 10^4 cells per well and grown in EGM-2 for 2 days. Then the cells were washed in Krebs-Ringer-Hepes (KRH) buffer (20 mM Hepes, 145 mM NaCl, 1.8 mM $CaCl_2$, 5.4 mM KCl, 1 mM $MgCl_2$, 0.8 mM Na_2PO_4, 5 mM glucose, pH 7.4) and incubated with 100 μM dichlorodihydrofluorescein diacetate (H_2DCF-DA; Molecular Probes) at 37°C for 30 minutes. After washing with KRH buffer, the cells were incubated at 37°C with 0.1 μM *t*-BHP or 10 μM BSO for 60 minutes in a Cytofluor 4000 plate reader. The fluorescence of 2′,7′-dichlorofluorescein (DCF), the oxidation product of H_2DCF, was detected under an excitation wavelength of 485±10 nm and an emission of 520±25 nm. Alternatively, after incubation with H_2DCF-DA, cultures were washed with ice-cold PBS, resuspended by trypsinization and analysed immediately using a FACScan flow cytometer (Becton Dickinson, Oxford, UK). Data were acquired and analysed with Cellquest software (Becton Dickinson). The DCF signal was measured on the FL1 detector and relative intracellular oxidant capacity was estimated using the median fluorescence intensity of the population.

Cell proliferation assay

Cell proliferation was determined using bromodeoxyuridine (BrdU) labelling. Cultures were incubated under normal or pro-oxidant conditions with 10 μg/ml BrdU and after various time intervals fixed in ethanol. Labelled cells were identified by immunocytochemistry using a mouse monoclonal antibody directed against BrdU (clone Bu20a), a biotinylated $F(Ab')_2$ fragment of rabbit anti-mouse immunoglobulin as the secondary reagent and streptavidin-horseradish peroxidase with diaminobenzidine for visualisation (all from DAKO, UK). Labelled cells were viewed with a Zeiss Axiovert 25 CFL inverted microscope and the percentage of positive cells was determined by counting at least 500 cells in each culture dish.

Cytochemical staining for SA-β-galactosidase

Cytochemical staining for senescence-associated β-galactosidase (SA-β-gal) was performed as previously described (Kurz et al., 2000).

Telomere length assay

Genomic DNA was extracted at the end of each passage and digested overnight at 37°C with *Hin*fI and *Rsa*I. Southern blot determination of mean terminal restriction fragment (TRF) length was performed using a biotinylated telomeric 51-mer oligonucleotide probe (BD Pharmingen, UK) at a concentration of 6.5 ng/ml. Hybridisation was

carried out at 65°C for 16 hours in hybridisation buffer (BD Pharmingen) followed by three 5-minute washes with 1× SSC/0.1% SDS at 42°C, and then three 15-minute washes with 0.1× SSC/0.1% SDS at 42°C. Hybridisation signals were detected by chemiluminescence and quantified by computer-assisted scanning densitometry using the public domain NIH Image software (version 1.62, available at http://rsb.info.nih.gov/nih-image). The mean TRF lengths were calculated by integrating the signal intensity over the entire TRF distribution as a function of TRF length using the formula TRF length=$\Sigma(OD_i) / \Sigma(OD_i/L_i)$, where OD_i and L_i are the signal intensity and TRF length respectively at position i on the autoradiogram.

Fluorescence in situ hybridisation (FISH)

HUVEC were treated overnight with 10 ng/ml colcemid followed by hypotonic swelling and fixation in 3:1 (v/v) methanol/acetic acid. Cell suspensions were then dropped onto slides, post-fixed with 70% acetic acid and dehydrated by passing through graded ethanol solutions following standard protocols. In situ hybridisation was performed using a fluorescein isothiocyanate (FITC)-conjugated $(CCCTAA)_3$ peptide nucleic acid probe (Perseptive Biosystems) as previously described (Lansdorp et al., 1996). Chromosomes were counterstained with 4′,6-diamidino-2-phenylindole (DAPI) and images of metaphase spreads were viewed by fluorescence microscopy. Images were captured using a cooled CCD camera (Photometrics) and Smartcapture software (Vysis). The fluorescence intensities of individual telomeres were calculated from the grey-scale digital images of the metaphase spreads after correction for background, using NIH Image software. Analysis of telomere length heterogeneity was performed by normalising the fluorescence intensity of each telomere spot to the median signal intensity of all telomeres in the metaphase spread.

*Bal*31 digestion

*Bal*31 digestion was carried out in 600 mM NaCl, 20 mM Tris-HCl, 12 mM $CaCl_2$, 12 mM $MgCl_2$ and 1 mM EDTA (pH 8.0) in a final volume of 25 μl containing 10 μg of genomic DNA and 0.25 units of *Bal*31 nuclease (New England Biolabs) at 30°C for various lengths of time. The reaction was stopped by addition of 3 μl 0.2 M EGTA and incubation for 10 minutes at 65°C. The digests were then extracted with 25/24/1 (v/v) phenol/chloroform/isoamyl alcohol, precipitated in ethanol, digested with *Hin*fI and *Rsa*I, and processed for Southern blot analysis of TRF length as described above.

Telomeric repeat amplification protocol (TRAP) assay

HUVEC were harvested by trypsinisation, counted using a haemocytometer, and lysed at 4°C in 3-[(3-cholamidopropyl)dimethylammonio]-1-propanesulfonic acid buffer. Aliquots of the cleared lysate equivalent to 2×10^4 cells were assayed for telomerase activity by a modified telomeric repeat amplification protocol (TRAPeze, Intergen, Oxford, UK), as previously described (Kurz et al., 2003). The activity of each sample was calculated from the ratio of the intensity of the telomeric repeat ladder (starting at 50 bp) to the 36 bp internal standard. Results, expressed in arbitrary units (AU), were normalized to the signal obtained from an extract of 500 HeLa cells routinely assayed in parallel as a positive control.

Detection of oxidised proteins and western blotting

Protein oxidation was analysed by immunoblot detection of carbonyl groups following derivatisation with 2,4-dinitrophenylhydrazine and using a commercially available detection system (Oxyblot, Oncor). Briefly, at the indicated passages 7.5×10^5 cells were extracted in 100 μl NP-40 lysis buffer (50 mM Tris-HCl pH 8, 150 mM NaCl, 1 mM EDTA, 1 mM Na_3VO_4, 1% NP-40, 5 mg/ml leupeptin, 1 mM PMSF) for 30 minutes on ice. Following centrifugation at 14,000 ***g*** for 30 minutes at 4°C, 1.5% β-mercaptoethanol was added to the supernatant, carbonyl group side chains were derivatised and proteins were separated by polyacrylamide gel electrophoresis. After transfer to PVDF membranes, oxidised proteins were identified by immunoblotting with antibodies against the dinitrophenyl moiety. Immunoreactive bands were detected using a horseradish peroxidase-labelled antibody and enhanced chemiluminescence. The relative intensity of each lane was quantified by scanning densitometry using NIH Image. Immunoblotting for hTERT was performed according to standard protocols using 50 μg of nuclear protein extract and a goat polyclonal antibody against the C terminus of hTERT (Santa Cruz Biotechnologies, CA, USA). Nuclear extracts were prepared as previously described (Andrews et al., 1991).

Immunostaining

Association of TRF1 with PML bodies was detected by immunofluorescent staining essentially as previously described (Wu et al., 2000). In brief, cells were grown on coverslips coated with 0.2% gelatine and then arrested in the G2/M phase of the cell cycle by incubation with 500 ng/ml nocodazole (Calbiochem) for 16 hours. Unless otherwise indicated all further incubations were carried out at room temperature. After washing with PBS, cells were fixed and permeabilised for 30 minutes with 3.7% formaldehyde in PBS containing 0.1% Triton X-100, followed by a further 30-minute incubation with 0.05% saponin in PBS. After five washes with PBS, coverslips were pre-treated with serum-free protein blocking reagent (DAKO) for 30 minutes and then incubated with primary antibodies for 1 hour. TRF1 was detected using a 1:1000 dilution of a goat polyclonal antibody raised against a peptide mapping to the amino terminus of human TRF1 (Santa Cruz Biotechnology), followed by a FITC-conjugated chicken anti-goat IgG (Molecular Probes, dilution 1:2000). Detection of the PML nuclear body was carried out using a 1:1000 dilution of a mouse monoclonal antibody raised against a peptide mapping to residues 37-51 of human PML (Santa Cruz Biotechnology), followed by Texas Red-conjugated rabbit anti-mouse IgG (Molecular Probes, 1:2000). A corresponding primary control antibody was used in each case as a negative control. After antibody staining, coverslips were washed extensively in PBS/0.5% Nonidet P-40 and nuclei were counterstained with 4′,6-diamidino-2-phenylindole (DAPI) in Vectashield mounting medium (Vector Laboratories). Immunofluorescence microscopy was performed with a Zeiss Axioskop Microscope using a 63×/1.4 NA Plan Apochromat objective and fluorescence filter sets appropriate for fluorescein, Texas Red and DAPI. Fluorescence images were acquired with a Hammatsu C4742-95 digital camera using Improvision acquisition and analysis software (Openlab, version 3).

Results

Low doses of *tert*-butyl hydroperoxide or L-buthionine sulphoximine increase the intracellular pro-oxidant status without causing cell toxicity

t-BHP, a substrate of glutathione peroxidase, and BSO, an inhibitor of γ-glutamyl cysteine synthase, are two compounds known to interfere with the glutathione-dependent antioxidant defences of the cell (Griffith and Meister, 1979; Jewell et al., 1986) (Fig. 1). In preliminary experiments these compounds were tested to find conditions that would cause chronic oxidative stress during long-term serial culture, without inducing cytotoxic effects. To this end, HUVEC were cultured for four passages in the presence of BSO or *t*-BHP at various doses. Viability assays using dual staining with calcein-AM

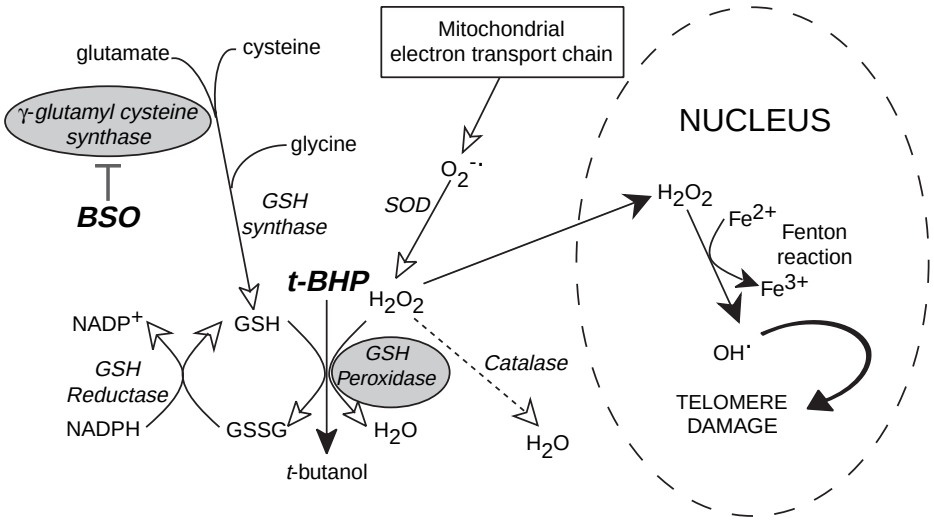

Fig. 1. Generation of oxidative stress by experimental interference with the metabolism of glutathione in human endothelial cells. Scheme depicting the central position of the glutathione redox-cycle in the intracellular detoxification of peroxides and the sites of pharmacological intervention used in this study (details in text). The proposed mechanism by which these alterations of redox homeostasis affect telomere integrity are shown. GSH, reduced glutathione; GSSG, oxidised glutathione; SOD, superoxide dismutase.

and ethidium homodimer-1 demonstrated that the highest concentrations of these compounds that could be used without inducing cell death were 0.1 μM *t*-BHP and 10 μM BSO (data not shown). These concentrations were thus chosen for subsequent experiments. Fig. 2A shows that under these conditions the intracellular oxidative capacity increased by 2.9±0.7-fold with *t*-BHP and by 2.2±0.3-fold with BSO. Labelling with BrdU during the first two passages demonstrated that under these pro-oxidant conditions there was a small but noticeable lengthening of the cell-cycle. Nevertheless, consistent with an absence of cytostatic or cytotoxic effects, there was no effect on the overall fraction of cells passing through S-phase (Fig. 2B). Taken together these results indicated that *t*-BHP and BSO might be used at low concentrations to cause chronic oxidative stress. In addition, immunoblot detection of protein carbonyl groups revealed a significant increase of intracellular protein oxidation in treated cultures (Fig. 2C), demonstrating that this mild oxidative treatment was biochemically effective also at the macromolecular level. Furthermore, the level of protein oxidation appeared to increase with treatment duration, although this was not statistically significant.

To investigate whether long-term pro-oxidant treatment affected the response to further oxidative insults, intracellular

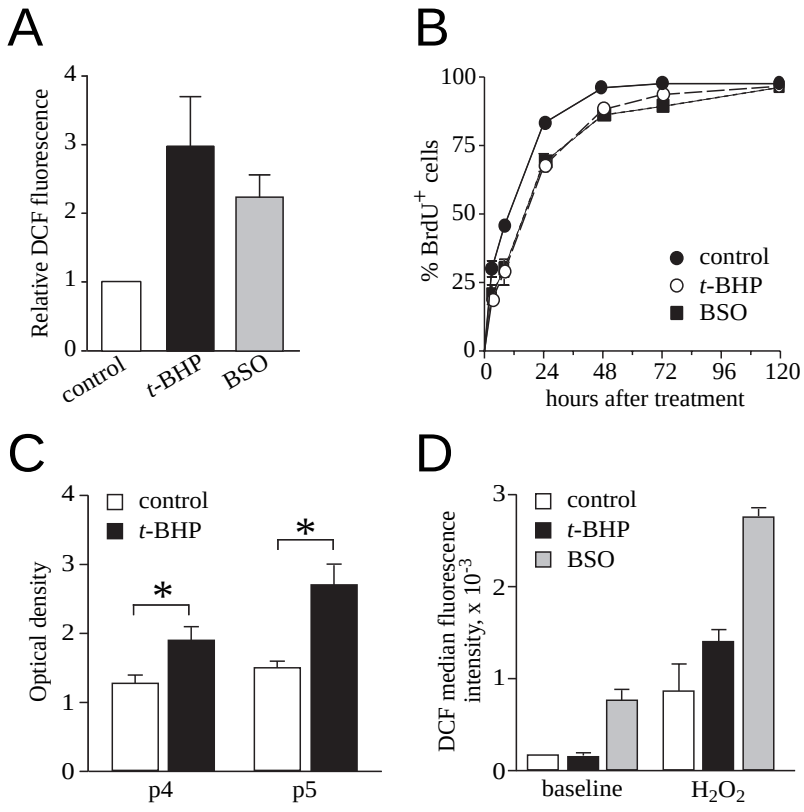

Fig. 2. Increase of the intracellular oxidant status by low concentrations of *t*-BHP or BSO without impairment of cell-cycle progression. (A) Intracellular pro-oxidant status was determined by fluorimetric detection of DCF. Values represent the increase in fluorescence recorded 30 minutes after addition of 0.1 μM *t*-BHP or 10 μM BSO, relative to the values recorded in control cells. Data are the mean (± s.d.) of triplicate wells from two experiments. (B) Cells were treated with 0.1 μM *t*-BHP (empty circles), 10 μM BSO (filled squares) or vehicle (filled circles) 48 hours after passage and simultaneously incubated with 10 μg/ml BrdU. Labelled cells were identified by immunocytochemistry at the indicated time points after treatment. Results represent the mean (± s.d.) of three replicate dishes from the third passage. (C) Whole cell lysates were prepared from cultures grown under control or pro-oxidant conditions during the fourth and fifth passage. Oxidised proteins were quantified as described in Materials and Methods. Results are the mean (± s.d.) of three replicate cultures. **P*<0.05. (D) Intracellular pro-oxidant status was determined by flow cytometry in late passage cultures (>25 CPD) before (baseline) and 30 minutes after addition of 200 μM H_2O_2. Values are the mean of three replicate dishes.

oxidant capacity was measured in late passage cultures before addition of the oxidant (at baseline) and immediately after treatment. As shown in Fig. 2D, baseline intracellular oxidative capacities in control and *t*-BHP-treated cultures (passage 11-12) were comparable, but in BSO-treated cultures (passage 8-10) were increased by approximately fourfold. This difference suggests that BSO induces a more sustained pro-oxidant state, presumably by causing a persistent depletion of glutathione stores, whereas *t*-BHP, being rapidly metabolised, has a transient effect. However, in both cases exposure to an oxidative challenge with hydrogen peroxide resulted in an increase in intracellular oxidative status of a similar or larger magnitude to that seen in untreated cells (Fig. 2D). This demonstrated that the response to further oxidant stress was not being blunted by adaptive mechanisms, but in contrast, persisted despite long-term culture under pro-oxidant conditions.

Chronic intracellular oxidative stress accelerates the onset of senescence

Long-term cultures maintained under normal conditions ceased to replicate after about 70 days, reaching 46 cumulative population doublings (CPD). In comparison, parallel cultures treated with *t*-BHP or BSO, continued to grow for a similar length of time but replicated at a slower rate (Fig. 3A). Evaluation of these cultures for senescence characteristics revealed that under these pro-oxidant conditions there was a premature decrease in cell density at confluence (Fig. 3B), an accelerated accumulation of SA-β-gal positive cells (Fig. 3C) and an increase in cell size (data not shown). Thus, cultures with a replicative age of only about 25-30 CPD grown under oxidative stress resembled senescent cultures of about 45 CPD grown under normal conditions.

Oxidative stress accelerates telomere attrition and induces long TRF species

Telomere restriction fragment analysis revealed that in HUVEC grown under normal conditions telomere erosion occurred at a constant rate of ~55 bp/PD and in a relatively uniform manner (Fig. 4A,B). In contrast, telomere shortening in cells cultured in the presence of *t*-BHP showed a biphasic behaviour. Initially, there was one population of telomeres, which, compared to control cultures, decreased in size at a much faster rate (~110 bp/PD). However, beginning at about 15-18 CPD, a more complicated pattern became evident involving two distinct TRF populations. One population consisted of the conventionally sized fragments, while the other population was composed of longer, more uniformly sized species. Both of these TRF species continued to decrease in size at similar rates (~110 bp/PD for conventional sized fragments and ~100 bp/PD for long fragments). It was noteworthy that when these long TRFs first appeared, they were larger than the longest conventional size TRFs from younger cultures, suggesting that some form of active telomere elongation had occurred. A similar pattern of telomere length changes was also found in cultures treated with BSO (Fig. 4C). These findings were reproducibly present in all HUVEC series grown under pro-oxidant conditions (three times *t*-BHP, two times BSO).

In order to investigate in more detail the nature of these long TRF species, telomeres were examined on metaphase spreads

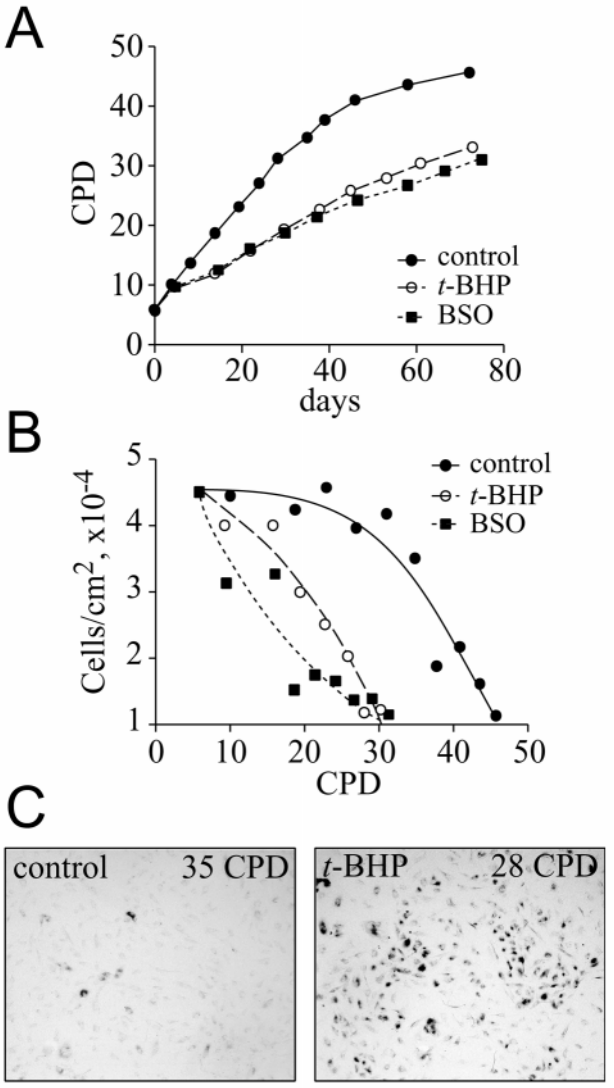

Fig. 3. Premature onset of senescence under chronic oxidative stress. (A) Long term growth curves of control and stressed cultures. (B) Cell density at confluence of control and stressed cultures as a function of CPD at each passage. (C) Brightfield photomicrographs showing senescence-associated β-galactosidase staining of control and stressed HUVECs at similar CPD levels.

of intermediate to late-passage cultures by FISH. Fig. 5A shows that telomeric signals from cells exposed to chronic oxidative stress were more heterogeneous than control cultures of similar replicative ages. Thus, while the majority of telomeric signals were clearly reduced, a minority appeared conspicuously brighter (Fig. 5A, arrows). The greater heterogeneity of telomere lengths within individual metaphases of cultures subjected to oxidant stress was confirmed by quantifying the relative fluorescence intensities of the individual telomere spots in ten representative examples each from control and *t*-BHP treated cells (Fig. 5B). Furthermore, histograms representing the cumulative frequency distributions of individual telomere fluorescence intensities demonstrated that a distinct subpopulation of long telomeres was present in oxidant-treated cultures, consistent with the results of the Southern blot analysis (Fig. 5C). These

findings also suggested that the appearance of long telomeres occurred in a subset of chromosomes within the majority of the treated cells.

We further considered the possibility that these long TRF species reflected chromosomal end-to-end fusions or other gross chromosomal abnormalities induced by telomere damage. Although FISH could not detect such aberrations in treated cells, we could not rule out that this was only because cells with these abnormalities would not progress through metaphase. Therefore, digestion of genomic DNA from late passage cultures with *Bal*31 nuclease prior to TRF analysis was undertaken. As shown in Fig. 6, the susceptibility of telomeres to *Bal*31 digestion was identical in DNA from all culture conditions, effectively ruling out the presence of chromosomal end-to-end fusions.

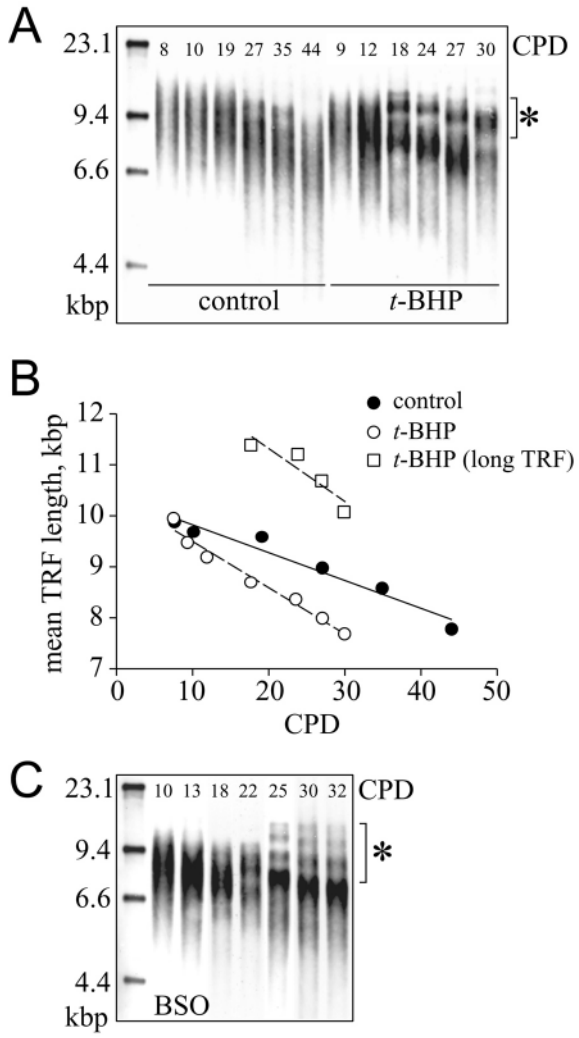

Fig. 4. Accelerated telomere attrition and appearance of long TRFs under chronic oxidative stress. (A,C) Southern blot hybridisation of a telomeric probe to genomic DNA from HUVEC of different replicative ages. A shows blots from cells were grown under normal conditions or chronically treated with 0.1 μM *t*-BHP during successive passages; C shows blots from cells treated with 10 μM BSO. Note in both cases the appearance of long TRF species (*) in the stressed cells at later passages. (B) The mean TRF lengths corresponding to the blots shown in A are plotted as a function of the replicative age.

Intracellular oxidative stress rapidly down-regulates telomerase activity

The possibility that the long TRF species represented a subpopulation of cells in which telomeres had been elongated as a result of telomerase reactivation was then considered. Consistent with previous reports (Vasa et al., 2000) cultures grown under normal conditions showed a decrease in

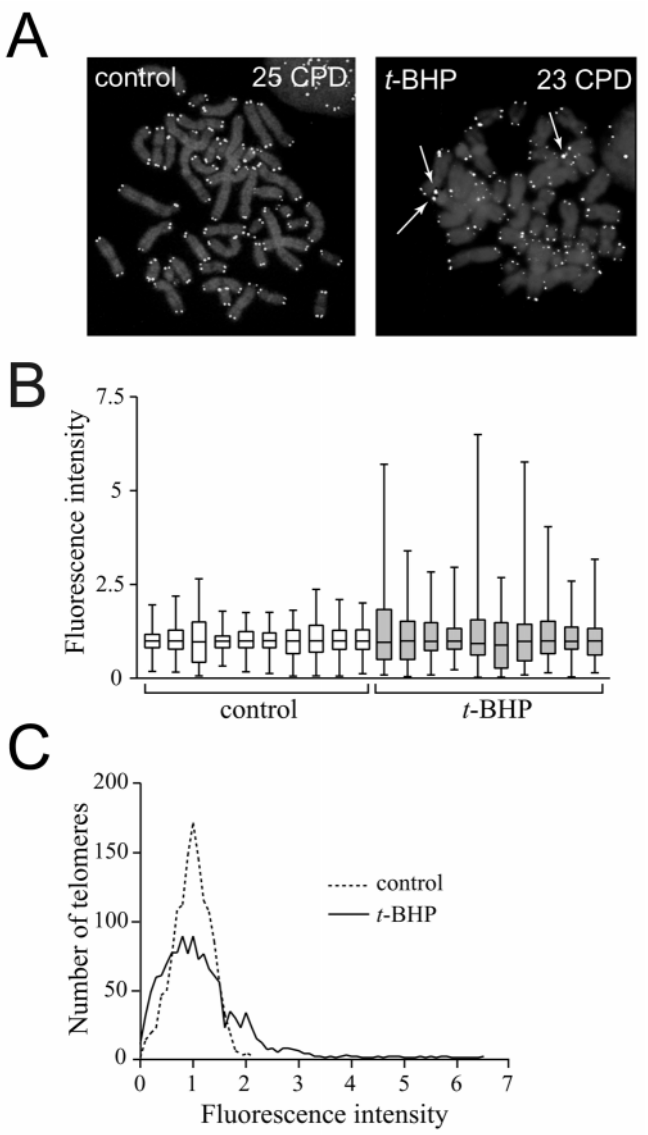

Fig. 5. Increased heterogeneity of TRF length under chronic oxidative stress. (A) FISH of a $(CCCTAA)_3$ telomeric probe to metaphase chromosomes from HUVEC of the indicated replicative ages after long term culture under pro-oxidant (*t*-BHP) or normal conditions. Photographs were taken using a 100× objective and identical exposure times. Note the bright telomeres (arrows) and the greater heterogeneity of signals in the *t*-BHP treated sample. (B) Box and whiskers plots for the relative telomere fluorescence intensities of ten representative metaphase spreads each of control and *t*-BHP-treated HUVEC cultures at 20-25 CPD. Boxes represent the spread of telomere signals between the 25th and 75th percentile, while bars show the range between the weakest and strongest telomere spot fluorescence. The horizontal line within the box represents the median. (C) Cumulative frequency distributions of all telomere signals from the metaphases shown in B.

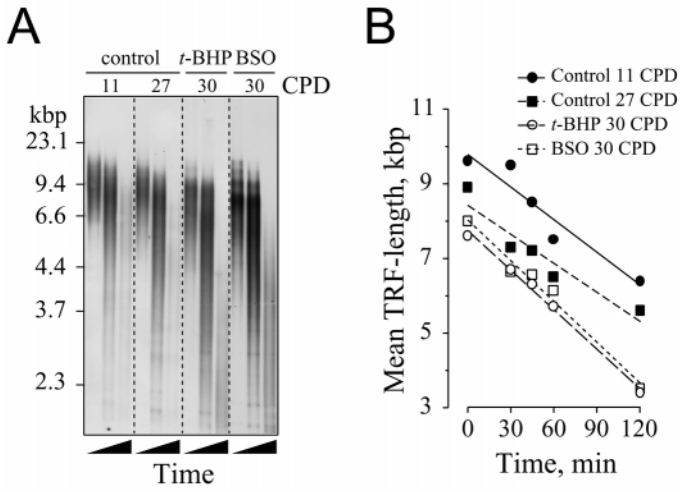

Fig. 6. Lack of evidence for chromosomal end-to-end fusions as the source of the long TRFs. (A) Time course of *Bal*31 exonuclease digestion of genomic DNA from HUVEC of the indicated replicative ages and culture conditions. Southern blot analysis for mean TRF length determination was performed as described in Fig. 4. The three lanes for each treatment are from samples digested with *Bal*31 for 30, 60 and 120 minutes, respectively. (B) The mean TRF length is plotted against the time of *Bal*31 digestion.

telomerase activity as a function of replicative age (Fig. 6A,B). Furthermore, in cultures grown under chronic oxidative stress telomerase activity was down regulated even faster, becoming virtually undetectable as early as 12 CPD (Fig. 6A,B). As shown in Fig. 6C, even the first oxidant treatment of HUVEC caused a very rapid (49% of control at 3 hours) and sustained (32% of control at 72 hours) decrease in telomerase activity. Furthermore, western blot analysis demonstrated that nuclear protein levels of hTERT, the catalytic subunit of telomerase, also decreased after the first oxidant treatment (Fig. 7D). Taken together, these results demonstrated that the decrease in telomerase activity caused by oxidative stress was not a consequence of premature senescence, but rather the result of a direct effect. Furthermore, these findings also indicate that appearance of long TRF species is not the outcome of telomerase up-regulation.

In search of evidence for the existence of ALT in HUVEC subjected to chronic oxidative stress

A pattern of increased telomere length heterogeneity within a single nucleus, similar to that found by us during long-term oxidant treatment has been demonstrated to be a characteristic of cell lines that use the 'alternative lengthening of telomeres' (ALT) mechanism of telomere maintenance (reviewed by Henson et al., 2002). These immortalised cells lack substantial telomerase activity and use instead recombinatorial mechanisms to maintain telomere length. In an attempt to find evidence for the existence of ALT in HUVEC subjected to chronic oxidative stress, we searched for the presence of PML bodies associating with telomeres in the nuclei of these cells. These structures have become known as 'ALT-associated PML bodies' (APBs), and have been repeatedly found to be present in ALT cell lines, where they colocalise with the telomere-associated proteins TRF1 and TRF2 (Henson et al., 2002). As shown in Fig. 8, PML bodies were readily visualised in HUVEC by immunofluorescence microscopy. However, neither TRF1 nor TRF2 could be detected by this method in either young control HUVEC or late passage HUVEC grown under pro-oxidant conditions (Fig. 8 and data not shown). In contrast, under the same experimental conditions, APBs were readily detected in the human ALT-positive osteosarcoma cell line U2OS (Fig. 8). In summary, these findings could neither support nor exclude a role for the ALT pathway in the generation of the long telomeres under oxidant culture conditions. Furthermore, they suggest that in HUVEC, the telomere-related proteins TRF1 and TRF2 are expressed at much lower levels than in immortalised cell lines.

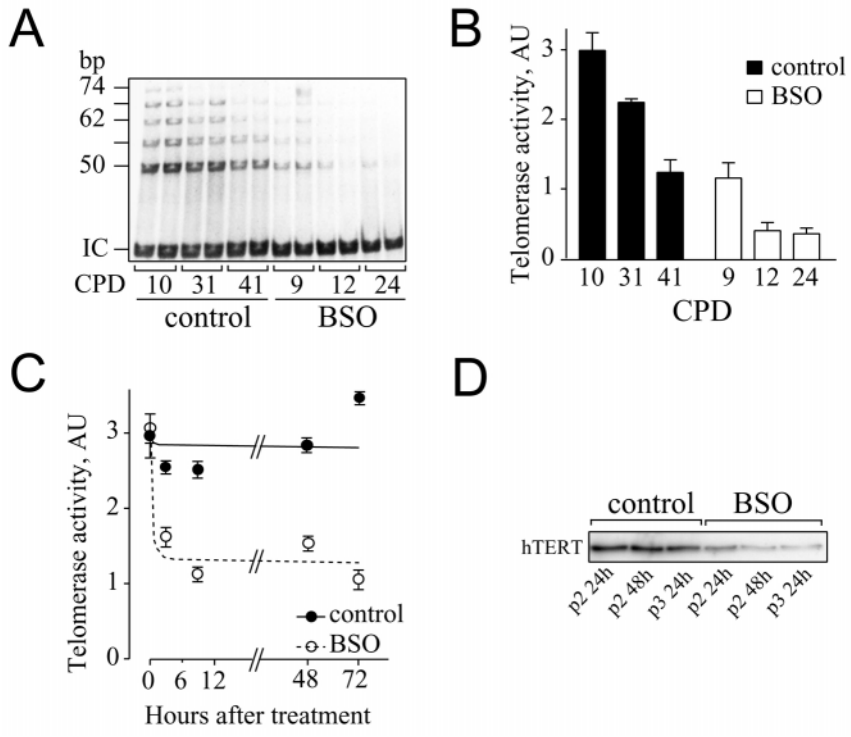

Fig. 7. Rapid decrease in telomerase activity following exposure to oxidative stress. (A,B) Comparison between telomerase activity levels in HUVEC of the indicated replicative ages cultured under pro-oxidant (BSO) or normal conditions. (A) TRAP products (≥50 base pairs); IC, internal polymerase chain reaction control in the TRAP assay. (B) Relative telomerase activity levels corresponding to the blots shown in A. (C) Time course of telomerase activity in young HUVEC (6 CPD) following a single exposure to 10 μM BSO. Values represent the mean (± s.d.) of duplicate cultures from representative experiments. (D) Immunoblots showing levels of hTERT in nuclear extracts at the indicated time points after the initial oxidant treatment at passage 2 and 3.

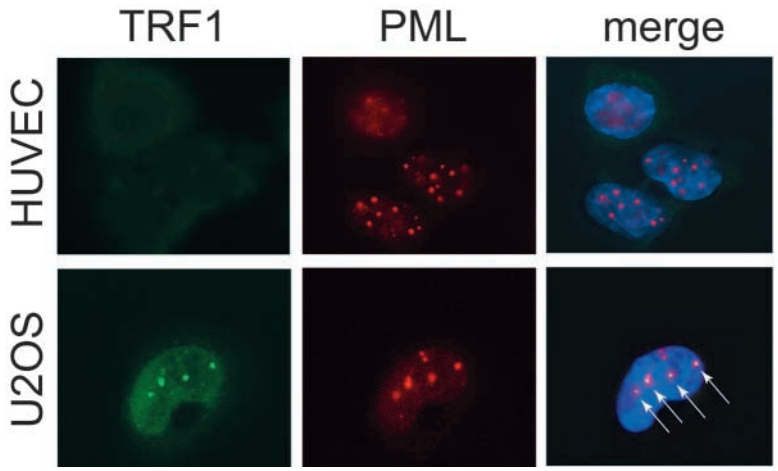

Fig. 8. In search of evidence for the existence of ALT in HUVEC subjected to chronic oxidative stress. Indirect immunofluorescence staining of TRF1 (green) and PML protein (red) in late passage HUVEC grown under pro-oxidant conditions (BSO) and in U2OS cells. Co-localisation of TRF1 and PML appears yellow (arrows). DNA was counterstained with DAPI (blue).

Discussion

The present study demonstrates that in normal endothelial cells mild chronic oxidative stress induced by interference with the glutathione-dependent anti-oxidant defences accelerates telomere erosion and the onset of replicative senescence. Furthermore, we show that under these pro-oxidant conditions, concomitantly with the faster telomere attrition, a distinct fraction of telomeres increase their length in the absence of telomerase activity. Our findings extend evidence from previous studies, the majority of which were performed in cultured fibroblasts (e.g. von Zglinicki et al., 1995; Petersen et al., 1998; Furumoto et al., 1998; Toussaint et al., 2000; Dumont et al., 2000; Xu et al., 2000; Chen et al., 2001; Tchirkov and Lansdorp, 2003) that have shown that both acute and chronic oxidative stress can induce a senescent phenotype. In a number of studies the premature onset of senescence has been further linked to accelerated telomere attrition (reviewed by von Zglinicki, 2002). However, the finding that oxidative stress leads to the emergence of abnormally long telomeres has not previously been reported.

In human endothelial cells the glutathione redox cycle has been shown to play a predominant role in the maintenance of redox homeostasis (Suttorp et al., 1986). Therefore, we chose to interfere with this system as a means to exert physiologically relevant oxidative stress. To this end, we used two distinct compounds, *t*-BHP and BSO, which are known to affect the metabolism of glutathione at different levels, namely utilisation (Jewell et al., 1986) and synthesis (Griffith and Meister, 1979), respectively. In preliminary experiments we set up culture conditions that would allow us to investigate the long-term effect of mild oxidative stress on telomere dynamics. To achieve this goal, it was essential to avoid acute growth arrest or cytotoxic cell death. In addition, since it has been shown that endothelial cells approaching senescence may undergo spontaneous apoptosis (Wagner et al., 2001; Zhang et al., 2002) it was necessary to define pro-oxidant culture conditions that would not enhance this propensity. By using significantly lower concentrations of *t*-BHP than those employed in other studies of senescence, we were able to induce a moderate, but effective increase in the intracellular oxidant capacity without causing cell death or cell cycle arrest (Fig. 2A-C). This allowed us to treat the cultures over several months through their whole replicative life span. We undertook a similar strategy with regards to the use of BSO, a substance that has not been employed previously in studies of telomere dynamics. Importantly, both compounds gave essentially identical results throughout the study, indicating that our findings were the consequence of effects related to the control of redox homeostasis.

The involvement of accelerated telomere erosion as a mechanism of stress-induced premature senescence has been a matter of debate (reviewed by von Zglinicki, 2002; Toussaint et al., 2002). In fibroblasts oxidant stress may induce or accelerate telomere shortening via generation of single strand breaks (Petersen et al., 1998). Conversely, it has been proposed that an apparent acceleration of telomere shortening may result from the compensatory expansion of a subpopulation of cells that escapes a stress-induced cell-cycle arrest (Dumont et al., 2001). In the present study, however, this possibility was ruled out by demonstrating in young cultures that cells did not drop from the cell cycle as a result of exposure to mild *t*-BHP or BSO treatment (Fig. 2B).

A major finding of this study was the discovery that a mild but chronic oxidative burden led to the emergence of distinct TRFs, which were longer and more uniform in size than the conventional TRF species (Fig. 4). Our initial assumption was that these long TRFs represented chromosomal end-to-end fusions, a phenomenon that has been documented in other models of telomere instability (Karlseder et al., 2002). This idea was further based on the fact that the long TRFs were approximately double the size of the shortest TRFs found in the same sample. However, both FISH and *Bal*31 digestion analysis could not confirm the presence of gross chromosomal abnormalities, making it a very unlikely source of the long TRF species (Fig. 5A, Fig. 6). We were also able to exclude the possibility that these long TRFs resulted from reactivation of telomerase activity (Fig. 7A,B). Indeed, in agreement with previous studies in HUVEC-treated with oxidised low density lipoprotein or H_2O_2 (Breitschopf et al., 2001), we found that oxidative stress generated by *t*-BHP or BSO in fact down-regulated telomerase in a rapid and persistent matter (Fig. 7C,D). It could be argued however, that up-regulation of telomerase was still occurring in a small subset of cells that could not be detected by the TRAP assay, and that this subpopulation might have been responsible for generating the long TRF species. However, evidence from the FISH analysis demonstrating increased telomere heterogeneity within the majority of the analysed cells did not support this possibility. One could further speculate that the reduction of telomerase activity may have contributed to the generation of these telomeric abnormalities. This hypothesis is consistent with more recent evidence suggesting that in human cells telomerase preserves telomere function and integrity independently of the maintenance of telomere length (Blasco, 2002; Masutomi et al., 2003).

A number of important differences between the present and other studies may explain why the emergence of long TRF species has not been found previously as a result of chronic oxidative stress. First, as stated above, a number of studies were performed with relatively high concentrations of oxidants, which most likely induce higher levels of macromolecular damage, preventing long-term cell culture. Second, the majority of studies were performed on fibroblasts, which are known to behave differently to endothelial cells with regard to their anti-oxidant defence mechanisms, their response to stress and their cell-cycle control (Michiels et al., 1990; Serrano and Blasco, 2001). Third, of the two studies performed on endothelial cells, one examined the effect of anti-oxidant rather than pro-oxidant treatment on telomere erosion (Furumoto et al., 1998), while the other, in which homocysteine was used to generate oxidative stress, did not examine the cultures beyond 15 population doublings (Xu et al., 2000).

It has been postulated that in the absence of telomerase activity telomeres can be elongated by recombinatorial mechanisms collectively known as 'alternative lengthening of telomeres' (ALT). Up until now, ALT activity has been found only in telomerase-deficient mouse cells and in human immortalised cell lines and tumours (reviewed by Henson et al., 2002). The present study suggests that recombinatorial mechanisms related to the ALT pathway might also be activated in normal cells when these are subjected to chronic oxidative stress, thus explaining the emergence of the long TRFs. This hypothesis is based on the fact that we have excluded the possibility of chromosomal end-to-end fusions or telomerase reactivation, and that oxidative stress is known to activate the DNA damage repair machinery (Zhou and Elledge, 2000). Indeed, there is some evidence suggesting that the DNA damage repair machinery may be mechanistically involved in the ALT pathway (Henson et al., 2002). In this context it should be emphasized that telomeres, on account of their guanine-rich composition, are several fold more susceptible to oxidative stress-mediated damage than non-telomeric DNA (Retel et al., 1993; Henle et al., 1999) and thus represent a prime site for recombinatorial events. The pattern of increased TRF heterogeneity within the same cell (Fig. 5A-C), a characteristic that has been suggested to be typical of cell lines that use the ALT pathway (Henson et al., 2002), would seem to support this concept. However, at present this possibility should be considered with caution. Indeed, since we were unable to identify the telomere-associated proteins TRF1 or TRF2 by immunofluorescence, we could neither confirm nor exclude the presence of ALT-associated PML bodies in our cultures. Furthermore, other characteristics indicate that HUVEC, with long TRF species, differ from ALT cell lines: (1) the long TRF species in HUVEC continued to decrease in length at a similar rate to the conventionally sized telomere population, whereas in ALT cell lines, these remain stable, and (2) no immortalisation was observed in our cultures. The fact that we could not detect TRF1 and TRF2 in HUVEC, whereas these proteins, and indeed APBs, were readily found in the ALT cell line U20S (Fig. 8), suggests that the levels of expression of these telomere binding proteins is much lower in HUVEC than in immortalised cells.

In summary, the following sequence of events is consistent with the findings of this study. (1) Persistent mild oxidative stress in replicating HUVEC accelerates telomere attrition and the loss of telomerase activity. (2) These events culminate in the disruption of telomere integrity and the consequent triggering of premature senescence. (3) In parallel to, and possibly facilitated by these effects, oxidative DNA damage induces the activation of the DNA damage repair machinery, facilitating recombinatorial events at the telomere, which will lengthen certain telomeres. It remains to be established whether cells in which telomeres have been elongated in this way would have their senescence time point reset and thus continue to replicate. At present we have no evidence suggesting that this process could lead to the immortalisation of endothelial cells.

The present findings may have important implications for the understanding of the relationship between ageing and the development of vascular pathologies. Studies from other laboratories have shown that telomeres in the vasculature shorten with age (Chang and Harley, 1995; Okuda et al., 2000; Aviv et al., 2001) and that this erosion is more pronounced in atherosclerosis-prone areas (Chang and Harley, 1995). In addition, we and others have shown that senescent endothelial cells are present in vivo in pathophysiological contexts (Fenton et al., 2001; Vasile et al., 2001; Minamino et al., 2002) known to be associated with increased oxidative stress (Griendling and Alexander, 1997). Our findings that glutathione-dependent redox homeostasis plays a pivotal role in the preservation of telomere integrity in endothelial cells suggest that perturbation of this system may be an important mechanism for oxidative stress-induced premature senescence of the endothelium and is entirely consistent with a role for telomere dysfunction in the pathogenesis of vascular disease.

This work was supported by grants from the Swiss National Science Foundation (D.J.K.), the Swiss Heart Foundation (D.J.K.) and the British Heart Foundation (S.D., Y.H. and J.D.E.). The authors wish to thank Dr Margareth Fox from the Department of Biology at UCL for her contribution to the FISH analysis of chromosomes.

References

Andrews, N. C. and Faller, D. V. (1991). A rapid micropreparation technique for extraction of DNA-binding proteins from limiting numbers of mammalian cells. *Nucleic Acids Res.* **19**, 2499.

Aviv, H., Khan, M. Y., Skurnick, J., Okuda, K., Kimura, M., Gardner, J., Priolo, L. and Aviv, A. (2001). Age dependent aneuploidy and telomere length of the human vascular endothelium. *Atherosclerosis* **159**, 281-287.

Blackburn, E. H. (2001). Switching and signaling at the telomere. *Cell* **106**, 661-673.

Blasco, M. A. (2002). Telomerase beyond telomeres. *Nat. Rev. Cancer* **2**, 627-633.

Bodnar, A. G., Ouellette, M., Frolkis, M., Holt, S. E., Chiu, C. P., Morin, G. B., Harley, C. B., Shay, J. W., Lichtsteiner, S. and Wright, W. E. (1998). Extension of life-span by introduction of telomerase into normal human cells. *Science* **279**, 349-352.

Breitschopf, K., Zeiher, A. M. and Dimmeler, S. (2001). Pro-atherogenic factors induce telomerase inactivation in endothelial cells through an Akt-dependent mechanism. *FEBS Lett.* **493**, 21-25.

Campisi, J. (1996). Replicative senescence: an old lives' tale? *Cell* **84**, 497-500.

Campisi, J., Kim, S. H., Lim, C. S. and Rubio, M. (2001). Cellular senescence, cancer and aging: the telomere connection. *Exp. Gerontol.* **36**, 1619-1637.

Celermajer, D. S., Sorensen, K. E., Spiegelhalter, D. J., Georgakopoulos, D., Robinson, J. and Deanfield, J. E. (1994). Aging is associated with endothelial dysfunction in healthy men years before the age-related decline in women. *J. Am. Coll. Cardiol.* **24**, 471-476.

Chang, E. and Harley, C. B. (1995). Telomere length and replicative aging in human vascular tissues. *Proc. Natl. Acad. Sci. USA* **92**, 11190-11194.
Chen, Q. M., Prowse, K. R., Tu, V. C., Purdom, S. and Linskens, M. H. (2001). Uncoupling the senescent phenotype from telomere shortening in hydrogen peroxide-treated fibroblasts. *Exp. Cell Res.* **265**, 294-303.
Collins, K. and Mitchell, J. R. (2002). Telomerase in the human organism. *Oncogene* **21**, 564-579.
Dayal, S., Brown, K. L., Weydert, C. J., Oberley, L. W., Arning, E., Bottiglieri, T., Faraci, F. M. and Lentz, S. R. (2002). Deficiency of glutathione peroxidase-1 sensitizes hyperhomocysteinemic mice to endothelial dysfunction. *Arterioscler. Thromb. Vasc. Biol.* **22**, 1996-2002.
Dumont, P., Burton, M., Chen, Q. M., Gonos, E. S., Frippiat, C., Mazarati, J. B., Eliaers, F., Remacle, J. and Toussaint, O. (2000). Induction of replicative senescence biomarkers by sublethal oxidative stresses in normal human fibroblast. *Free Radic. Biol. Med.* **28**, 361-373.
Dumont, P., Royer, V., Pascal, T., Dierick, J. F., Chainiaux, F., Frippiat, C., de Magalhaes, J. P., Eliaers, F., Remacle, J. and Toussaint, O. (2001). Growth kinetics rather than stress accelerate telomere shortening in cultures of human diploid fibroblasts in oxidative stress-induced premature senescence. *FEBS Lett.* **502**, 109-112.
Fenton, M., Barker, S., Kurz, D. J. and Erusalimsky, J. D. (2001). Cellular senescence after single and repeated balloon catheter denudations of rabbit carotid arteries. *Arterioscler. Thromb. Vasc. Biol.* **21**, 220-226.
Finkel, T. and Holbrook, N. J. (2000). Oxidants, oxidative stress and the biology of ageing. *Nature* **408**, 239-247.
Furumoto, K., Inoue, E., Nagao, N., Hiyama, E. and Miwa, N. (1998). Age-dependent telomere shortening is slowed down by enrichment of intracellular vitamin C via suppression of oxidative stress. *Life Sci.* **63**, 935-948.
Griendling, K. K. and Alexander, R. W. (1997). Oxidative stress and cardiovascular disease. *Circulation* **96**, 3264-3265.
Griffith, O. W. and Meister, A. (1979). Potent and specific inhibition of glutathione synthesis by buthionine sulfoximine (S-n-butyl homocysteine sulfoximine). *J. Biol. Chem.* **254**, 7558.
Hayflick, L. (1965). The limited in vitro life time of human diploid cell strains. *Exp. Cell Res.* **37**, 614-636.
Henle, E. S., Han, Z., Tang, N., Rai, P., Luo, Y. and Linn, S. (1999). Sequence-specific DNA cleavage by Fe2+-mediated Fenton reactions has possible biological implications. *J. Biol. Chem.* **274**, 962-971.
Henson, J. D., Neumann, A. A., Yeager, T. R. and Reddel, R. R. (2002). Alternative lengthening of telomeres in mammalian cells. *Oncogene* **21**, 598-610.
Jewell, S. A., Di Monte, D., Richelmi, P., Bellomo, G. and Orrenius, S. (1986). tert-Butylhydroperoxide-induced toxicity in isolated hepatocytes: contribution of thiol oxidation and lipid peroxidation. *J. Biochem. Toxicol.* **1**, 13-22.
Karlseder, J., Smogorzewska, A. and de Lange, T. (2002). Senescence induced by altered telomere state, not telomere loss. *Science* **295**, 2446-2449.
Kurz, D. J., Decary, S., Hong, Y. and Erusalimsky, J. D. (2000). Senescence-associated beta-galactosidase reflects an increase in lysosomal mass during replicative ageing of human endothelial cells. *J. Cell Sci.* **113**, 3613-3622.
Kurz, D. J., Hong, Y., Trivier, E., Huang, H. L., Decary, S., Zang, G. H., Luscher, T. F. and Erusalimsky, J. D. (2003). Fibroblast growth factor-2, but not vascular endothelial growth factor, upregulates telomerase activity in human endothelial cells. *Arterioscler. Thromb. Vasc. Biol.* **23**, 748-754.
Lakatta, E. G. and Levy, D. (2003). Arterial and cardiac aging: major shareholders in cardiovascular disease enterprises: Part I: aging arteries: a "set up" for vascular disease. *Circulation* **107**, 139-146.
Lansdorp, P. M., Verwoerd, N. P., van de Rijke, F. M., Dragowska, V., Little, M. T., Dirks, R. W., Raap, A. K. and Tanke, H. J. (1996). Heterogeneity in telomere length of human chromosomes. *Hum. Mol. Genet.* **5**, 685-691.
Levesque, A., Paquet, A. and Page, M. (1995). Measurement of tumor necrosis factor activity by flow cytometry. *Cytometry* **20**, 181-184.
Masutomi, K., Yu, E. Y., Khurts, S., Ben-Porath, I., Currier, J. L., Metz, G. B., Brooks, M. W., Kaneko, S., Murakami, S., DeCaprio, J. A., Weinberg, R. A., Stewart, S. A. and Hahn, W. C. (2003). Telomerase maintains telomere structure in normal human cells. *Cell* **114**, 241-253.
Michiels, C., Toussaint, O. and Remacle, J. (1990). Comparative study of oxygen toxicity in human fibroblasts and endothelial cells. *J. Cell Physiol.* **144**, 295-302.
Minamino, T., Miyauchi, H., Yoshida, T., Ishida, Y., Yoshida, H. and Komuro, I. (2002). Endothelial cell senescence in human atherosclerosis: role of telomere in endothelial dysfunction. *Circulation* **105**, 1541-1544.
Okuda, K., Khan, M. Y., Skurnick, J., Kimura, M., Aviv, H. and Aviv, A. (2000). Telomere attrition of the human abdominal aorta: relationships with age and atherosclerosis. *Atherosclerosis* **152**, 391-398.
Petersen, S., Saretzki, G. and von Zglinicki, T. (1998). Preferential accumulation of single-stranded regions in telomeres of human fibroblasts. *Exp. Cell Res.* **239**, 152-160.
Retel, J., Hoebee, B., Braun, J. E., Lutgerink, J. T., van den, A. E., Wanamarta, A. H., Joenje, H. and Lafleur, M. V. (1993). Mutational specificity of oxidative DNA damage. *Mutat. Res.* **299**, 165-182.
Rivard, A., Fabre, J. E., Silver, M., Chen, D., Murohara, T., Kearney, M., Magner, M., Asahara, T. and Isner, J. M. (1999). Age-dependent impairment of angiogenesis. *Circulation* **99**, 111-120.
Serrano, M. and Blasco, M. A. (2001). Putting the stress on senescence. *Curr. Opin. Cell Biol.* **13**, 748-753.
Smogorzewska, A. and de Lange, T. (2002). Different telomere damage signaling pathways in human and mouse cells. *EMBO J.* **21**, 4338-4348.
Strong, J. P. and McGill, H. C., Jr (1962). The natural history of coronary atherosclerosis. *Am. J. Pathol.* **40**, 37-49.
Suttorp, N., Toepfer, W. and Roka, L. (1986). Antioxidant defence mechanisms of endothelial cells: glutathione redox cycle versus catalase. *Am. J. Physiol.* **251**, C671-C680.
Tchirkov, A. and Lansdorp, P. M. (2003). Role of oxidative stress in telomere shortening in cultured fibroblasts from normal individuals and patients with ataxia-telangiectasia. *Hum. Mol. Genet.* **12**, 227-232.
Toussaint, O., Medrano, E. E. and von Zglinicki, T. (2000). Cellular and molecular mechanisms of stress-induced premature senescence (SIPS) of human diploid fibroblasts and melanocytes. *Exp. Gerontol.* **35**, 927-945.
Toussaint, O., Remacle, J., Dierick, J. F., Pascal, T., Frippiat, C., Zdanov, S., Magalhaes, J. P., Royer, V. and Chainiaux, F. (2002). From the Hayflick mosaic to the mosaics of ageing. Role of stress-induced premature senescence in human ageing. *Int. J. Biochem. Cell Biol.* **34**, 1415-1429.
van der Loo, B., Labugger, R., Skepper, J. N., Bachschmid, M., Kilo, J., Powell, J. M., Palacios-Callender, M., Erusalimsky, J. D., Quaschning, T., Malinski, T. et al. (2000). Enhanced peroxynitrite formation is associated with vascular aging. *J. Exp. Med.* **192**, 1731-1744.
Vasa, M., Breitschopf, K., Zeiher, A. M. and Dimmeler, S. (2000). Nitric oxide activates telomerase and delays endothelial cell senescence. *Circ. Res.* **87**, 540-542.
Vasile, E., Tomita, Y., Brown, L. F., Kocher, O. and Dvorak, H. F. (2001). Differential expression of thymosin beta-10 by early passage and senescent vascular endothelium is modulated by VPF/VEGF: evidence for senescent endothelial cells in vivo at sites of atherosclerosis. *FASEB J.* **15**, 458-466.
von Zglinicki, T. (2002). Oxidative stress shortens telomeres. *Trends Biochem. Sci.* **27**, 339-344.
von Zglinicki, T., Saretzki, G., Docke, W. and Lotze, C. (1995). Mild hyperoxia shortens telomeres and inhibits proliferation of fibroblasts: a model for senescence? *Exp. Cell Res.* **220**, 186-193.
Wagner, M., Hampel, B., Bernhard, D., Hala, M., Zwerschke, W. and Jansen-Durr, P. (2001). Replicative senescence of human endothelial cells in vitro involves G1 arrest, polyploidization and senescence-associated apoptosis. *Exp. Gerontol.* **36**, 1327-1347.
Weingand, K. W., Clarkson, T. B., Adams, M. R. and Bostrom, A. D. (1986). Effects of age and/or puberty on coronary artery atherosclerosis in cynomolgus monkeys. *Atherosclerosis* **62**, 137-144.
Weinsaft, J. W. and Edelberg, J. M. (2001). Aging-associated changes in vascular activity: a potential link to geriatric cardiovascular disease. *Am. J. Geriatr. Cardiol.* **10**, 348-354.
Wu, G., Lee, W. H. and Chen, P. L. (2000). NBS1 and TRF1 colocalize at promyelocytic leukemia bodies during late S/G2 phases in immortalized telomerase-negative cells. Implication of NBS1 in alternative lengthening of telomeres. *J. Biol. Chem.* **275**, 30618-30622.
Xu, D., Neville, R. and Finkel, T. (2000). Homocysteine accelerates endothelial cell senescence. *FEBS Lett.* **470**, 20-24.
Zhang, J., Patel, J. M. and Block, E. R. (2002). Enhanced apoptosis in prolonged cultures of senescent porcine pulmonary artery endothelial cells. *Mech. Ageing Dev.* **123**, 613-625.
Zhou, B. B. and Elledge, S. J. (2000). The DNA damage response: putting checkpoints in perspective. *Nature* **408**, 433-439.